Supplementary Information

Reconciling contrasting views on economic complexity

SCIARRA ET AL.

CONTENTS

SUPPLEMENTARY FIGURES

SUPPLEMENTARY FIGURE 1

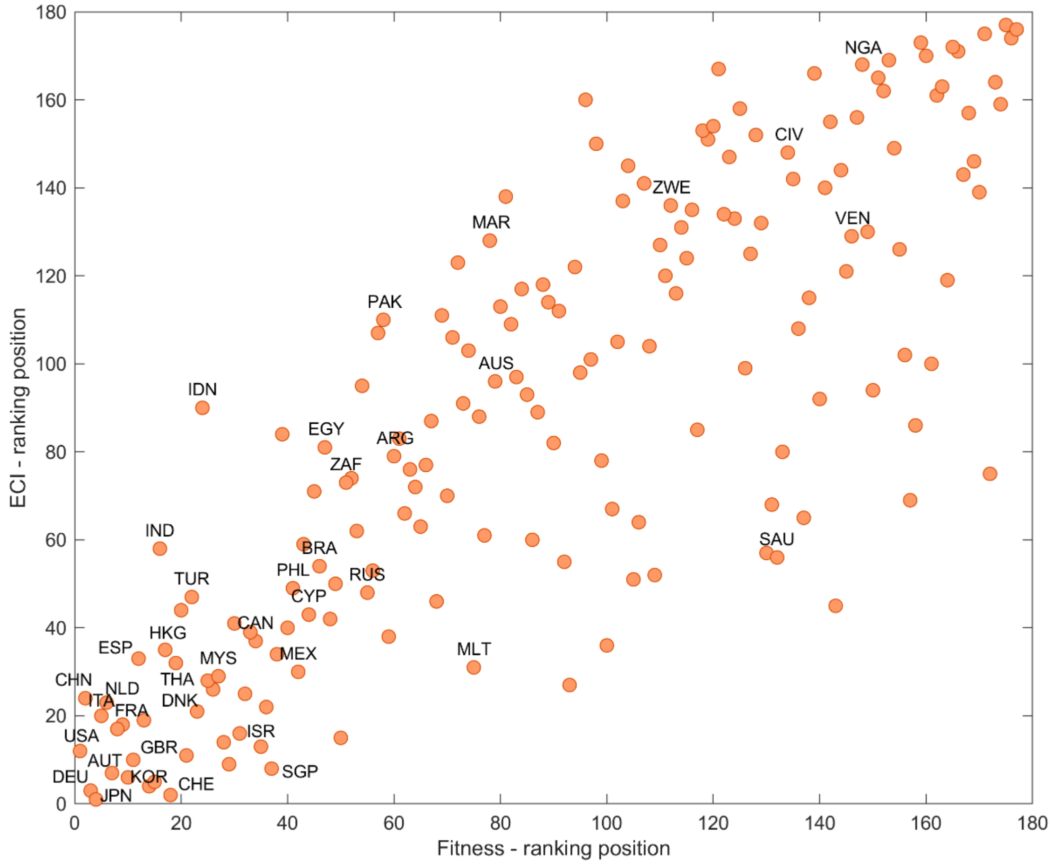

Comparison between the rankings provided by the Fitness and the ECI values. The rankings sort countries according to decreasing complexity, as computed by the two metrics. Results refer to year 2017.

SUPPLEMENTARY FIGURE 2

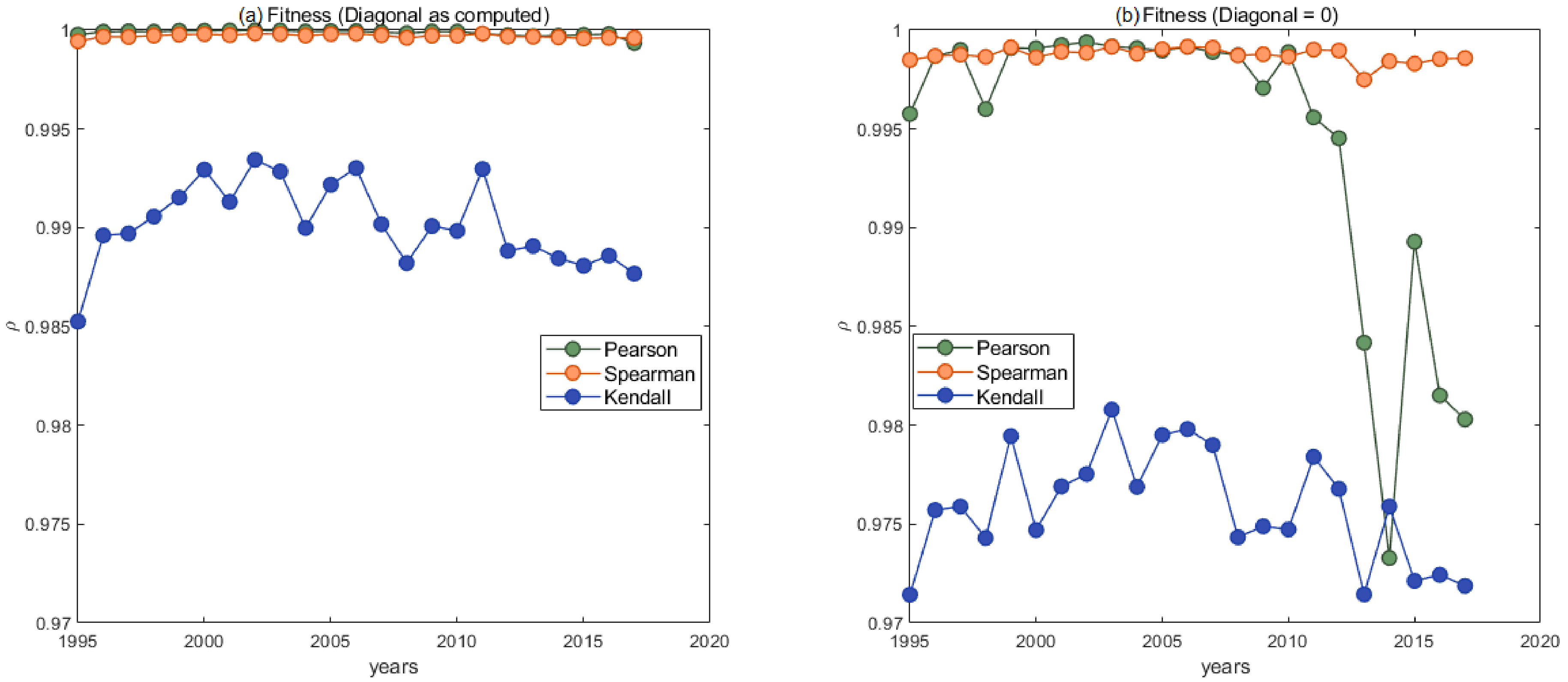

Correlation coefficients among the non-linearly and the linearly computed values of Fitness. In green is Pearson's correlation coefficient, while Spearman's one is in orange and Kendall's in blue. The Spearman's and Kendall's coefficients are ranking-based, while the Pearson's one compares the values between the two vectors. In panel (a), the results refer to the case in which the diagonal values of the matrix **N** are left as computed. In panel (b), the results refer to the case in which the diagonal values of the matrix **N** are set to zero. The FC iterative method has been implemented according to the directives in *(1)* (see Methods, Eqs 11). The linearised algorithm almost perfectly reproduces the outcomes of the non-linear one, whether or not the diagonal values are modified from the computed ones (panels (a) and (b), respectively; see Methods, Eq 15).

SUPPLEMENTARY FIGURE 3

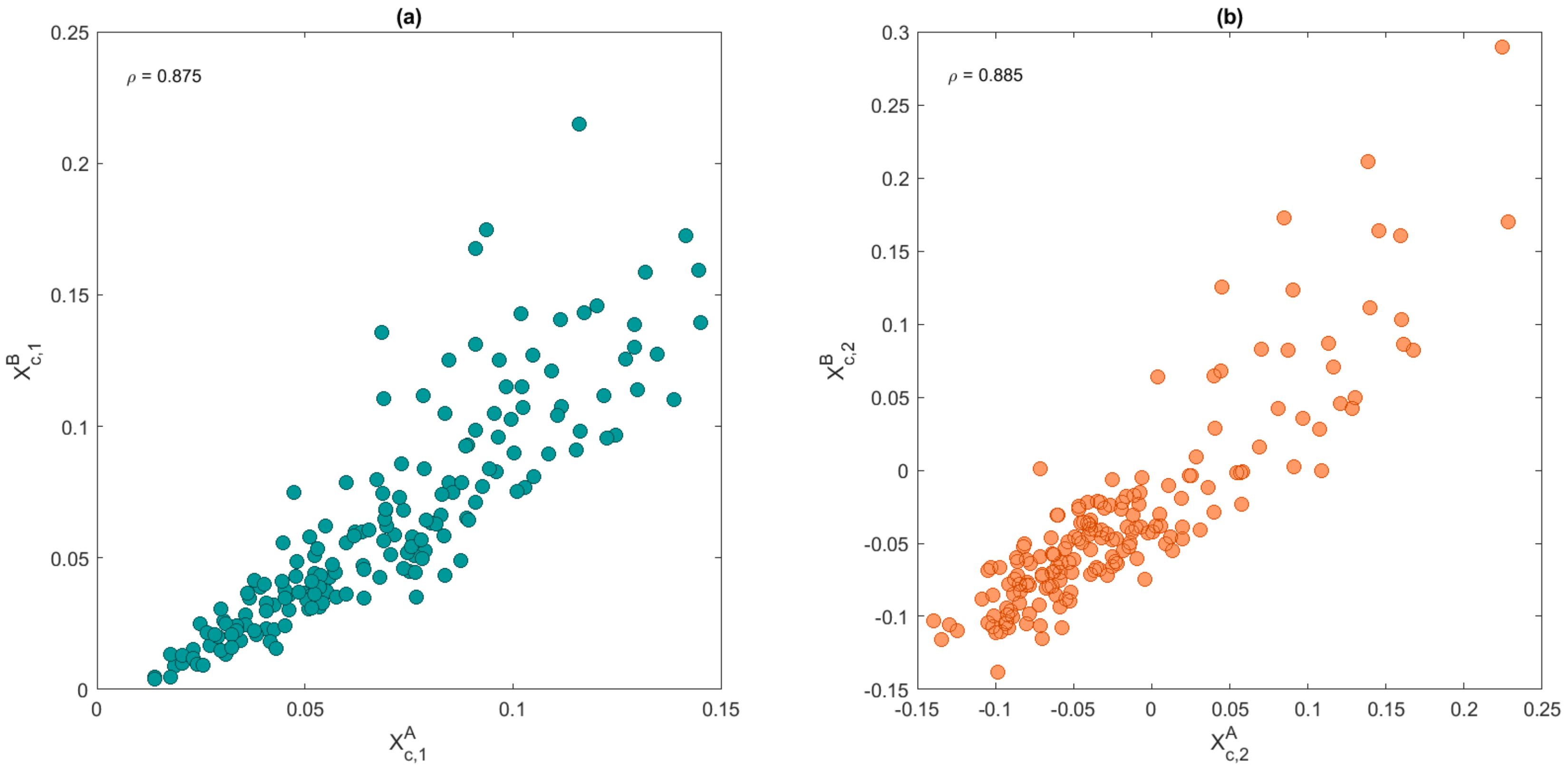

Scatter plots comparing the eigenvectors of the proximity matrices N^A and N^B . The matrices are computed using the transformation matrices $W^A_{cp} = \frac{M_{cp}}{\sqrt{k_c k_p}}$ and $W^B_{cp} = \frac{M_{cp}}{k_c k'_p}$ respectively. The left plot (a) compares the eigenvectors $X^A_{c,1}$ and $X^B_{c,1}$ associated to the largest eigenvalues λ^A_1 and λ^B_1 of the two proximity matrices, N^A and N^B. The right plot (b) compares the eigenvectors corresponding to the second largest eigenvalues λ^A_2 and λ^B_2, namely $X^A_{c,2}$ and $X^B_{c,2}$. The eigenvectors are normalized such that the Frobenius norm is unitary, i.e., $\sqrt{\sum_c X^2_{c,i}} = 1,\ (i = 1,2)$. As detailed in the main text, and as the correlation coefficients highlight, the eigenvectors from the two matrices carry similar information. The correlation coefficients are of the Pearson's kind.

SUPPLEMENTARY FIGURE 4

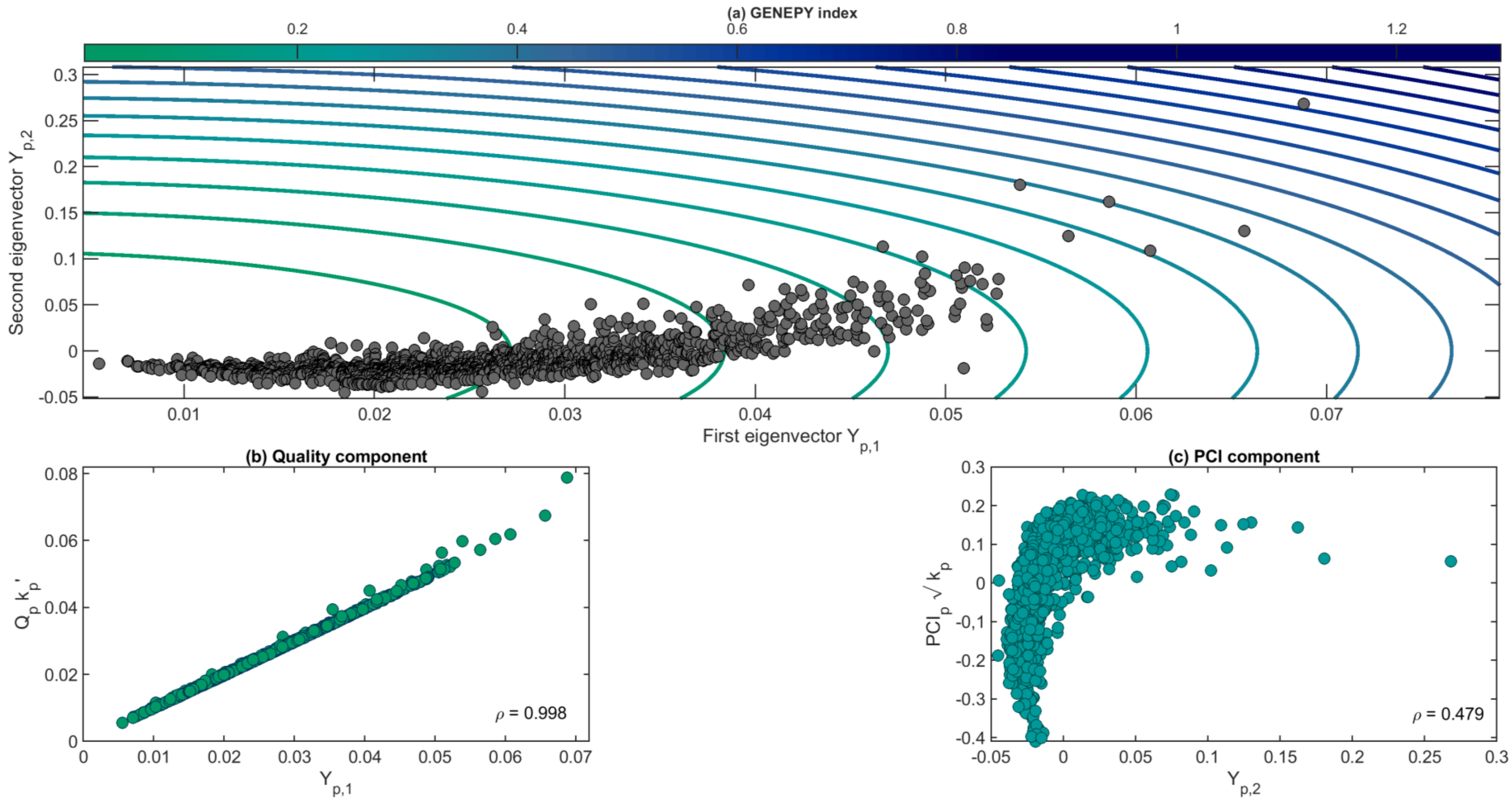

Products' GENEPY results and components as referred to the 2017 international commodities trade. (a) Contour plot of the GENEPY values. We interpret increasing economic complexity with increasing radial distance from the origin. The x-axis reports the values of the first eigenvector $Y_{p,1}$ whilst the y-axis the values of the second eigenvector $Y_{p,2}$. The eigenvectors are normalized such that their Frobenius norm is unitary, i.e., $\sqrt{\sum_p Y_{p,i}^2} = 1$, with $(i = 1,2)$. Contours range from lower GENEPY values (green) to higher ones (blue). (b) Scatter plot of the first component $Y_{p,1}$ of GENEPY values compared with the values of the Quality values Q_p rescaled by the products corrected degree k_p'. (c) Scatter plot of the second component $Y_{p,2}$ of GENEPY compared with PCI values, rescaled by the term $\sqrt{k_p}$. The correlation coefficients are of the Pearson's kind. This year totaled 1232 traded commodities.

SUPPLEMENTARY FIGURE 54

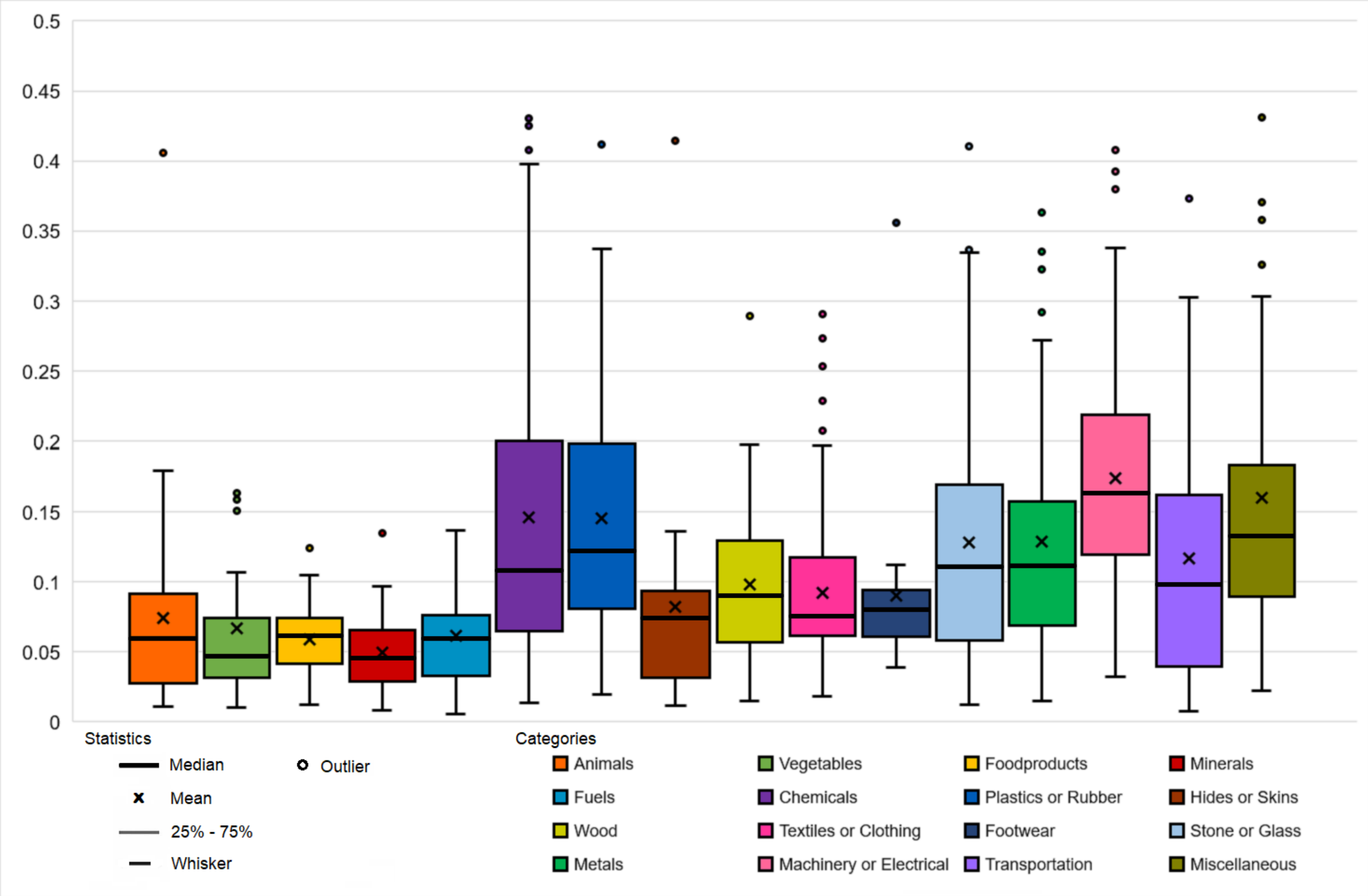

Boxplots of the GENEPY values for products aggregated into categories. Categories are defined as according to *(6)*. In the boxplot the cross is the mean, the thick bar is the median, the bars define the interquartile range (IQR) 25% - 75%, the shorter bars are the whiskers and the dots are outliers. From above the upper quartile, a distance of 1.5 times the IQR is measured out and a whisker is drawn up to the largest observed point from the dataset that falls within this distance. Similarly, a distance of 1.5 times the IQR is measured out below the lower quartile and a whisker is drawn up to the lower observed point from the dataset that falls within this distance. All other observed points are plotted as outliers.

SUPPLEMENTARY FIGURE 6

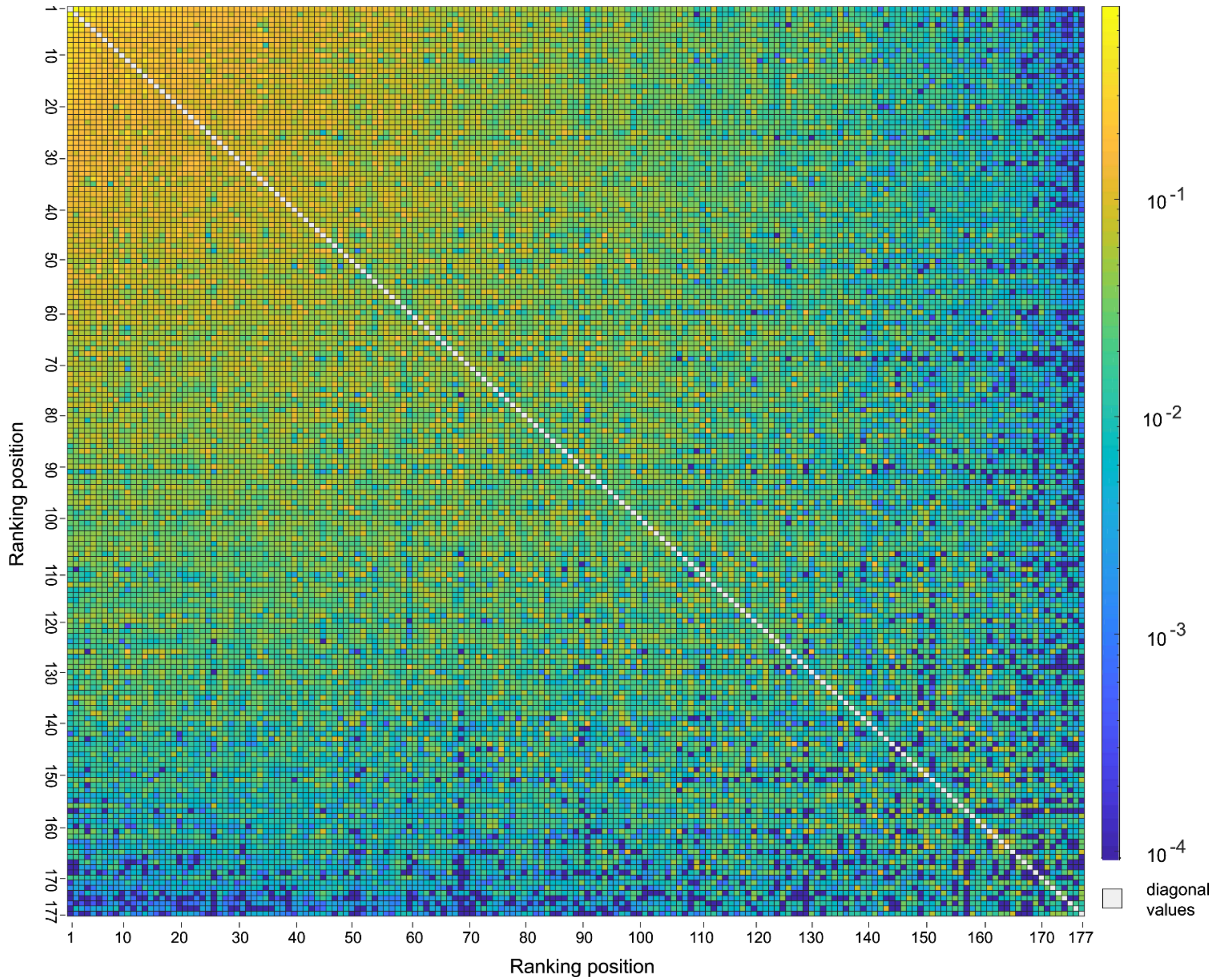

The elements N_{cc^*} of the similarity matrix N for the 2017 trade. Rows and columns reordered top-to-bottom, left-to-right, according to decreasing values of GENEPY complexity. More complex countries are found on the top (left) of the matrix. Correspondence among ranking positions and countries are defined in Supplementary Table 1.

SUPPLEMENTARY FIGURE 7

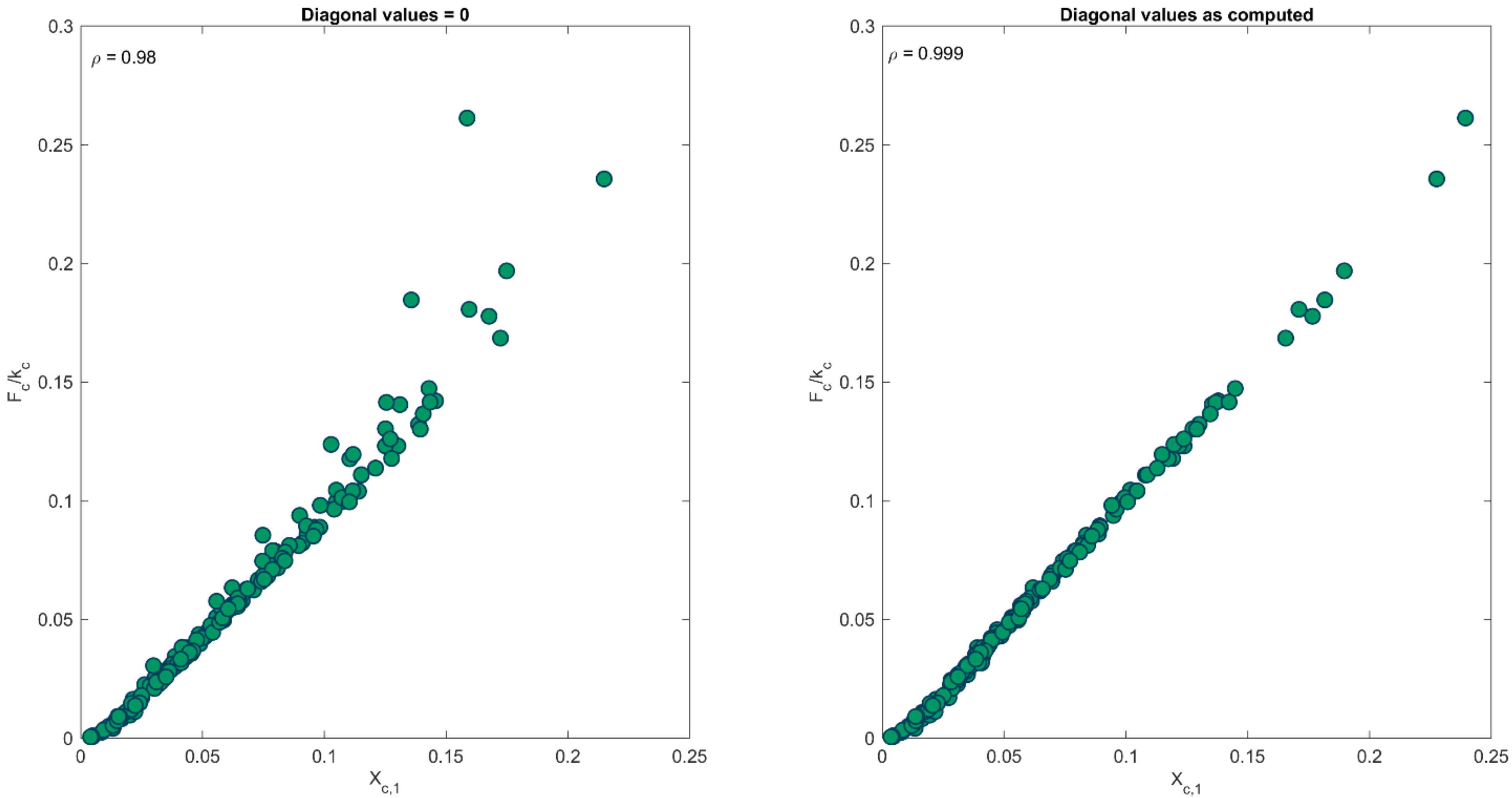

Scatter plots of the eigenvectors $X_{c,1}$ and F_c/k_c for different interpretations of the matrix N. On the left, the eigenvector $X_{c,1}$ belongs to the matrix N with diagonal values set to zero. On the right, $X_{c,1}$ is the eigenvector of the matrix N in which we left the diagonal values as computed, i.e., $N_{cc} = \sum_p M_{cp} M_{c^*p} \,/\, k_c k_c (k'_p)^2$ (see Methods, Eq 15). Data refer to year 2017.

Supplementary Figure 8

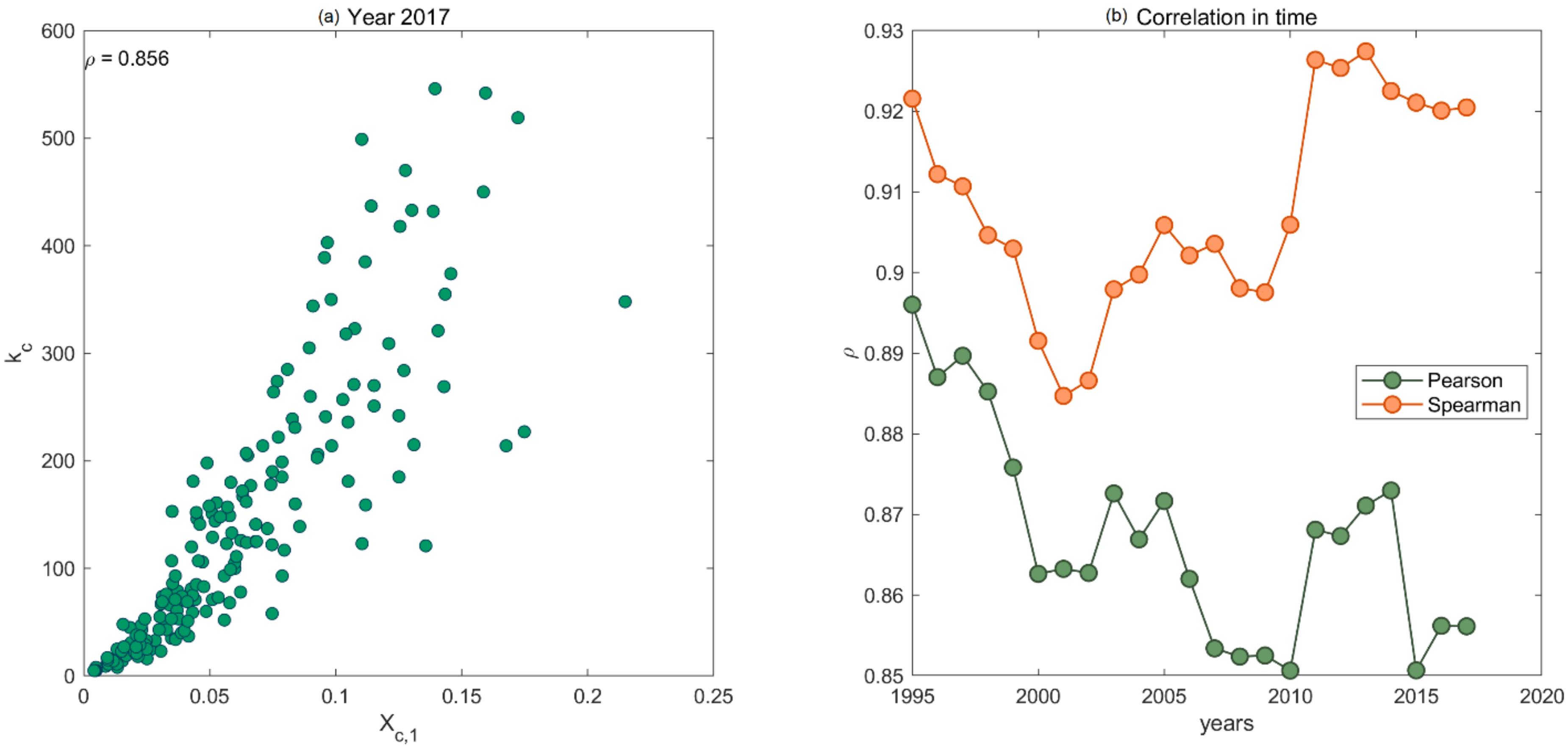

Correlation between $X_{c,1}$ and k_c. In panel (a), the scatter plot of the values from year 2017. In panel (b), the values of the correlation coefficients between the two vectors during time. The correlation of the Pearson's kind is in green, while the Spearman's one in orange.

SUPPLEMENTARY FIGURE 9

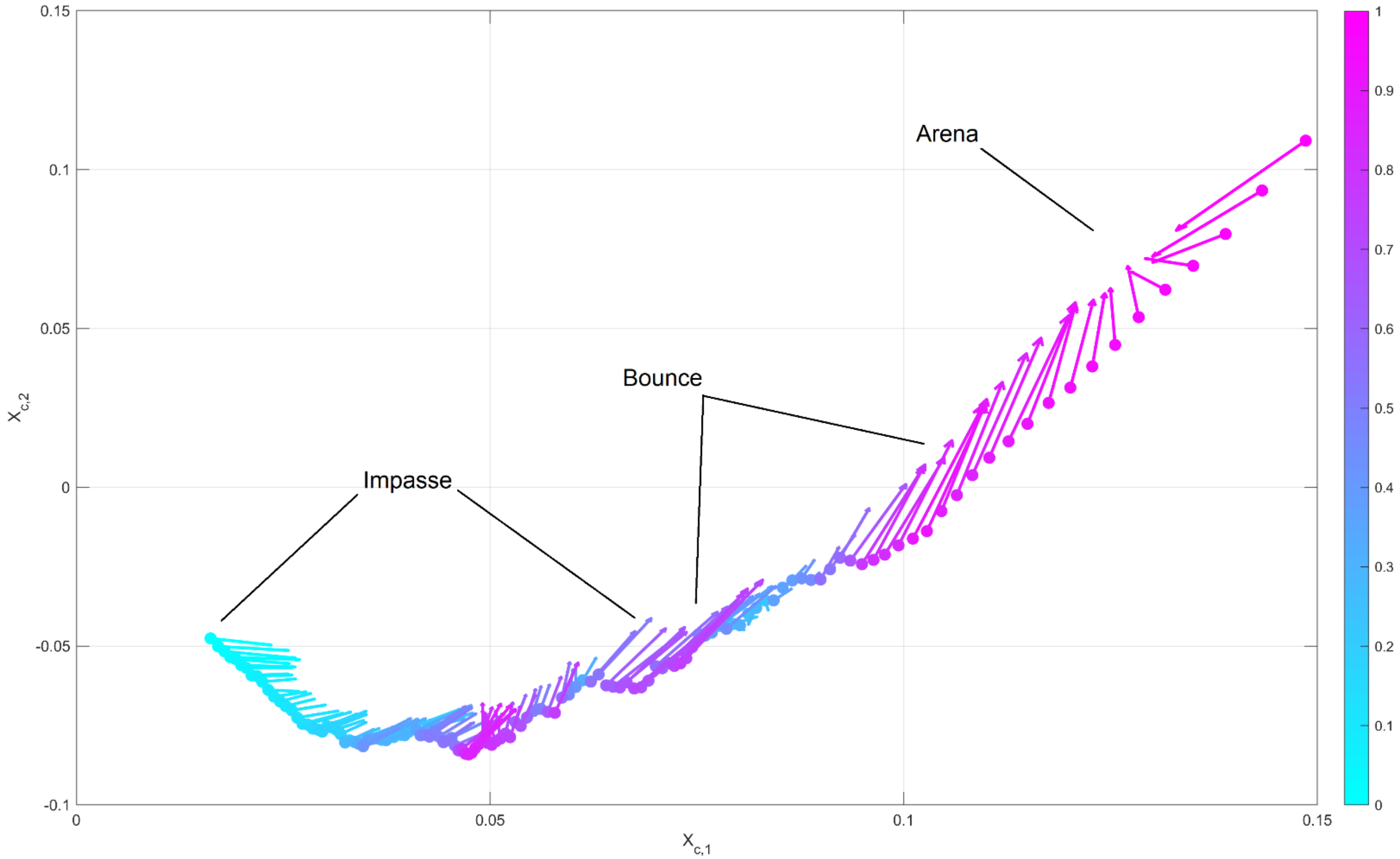

The time regimes of economic growth according to the two contributions $X_{c,1}$ and $X_{c,2}$. During time, countries move along the knee-like shape designed by the arrows.

SUPPLEMENTARY FIGURE 10

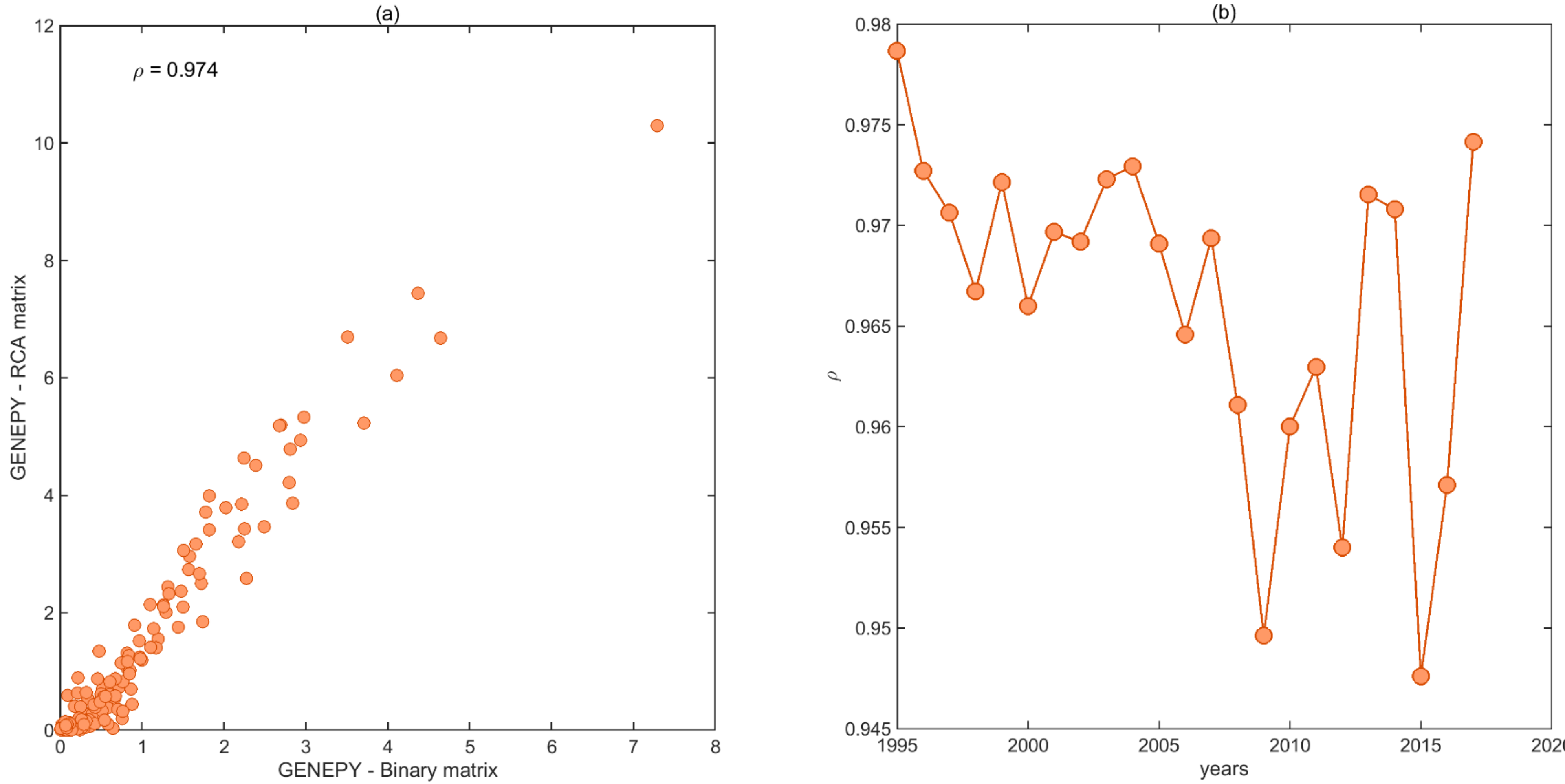

Comparison of the GENEPY of countries computed using either binary or RCA matrix. (a) Scatter plot of the GENEPY index as obtained from the use of the binary matrix M – on the x-axis – and from the RCA matrix – on the y-axis – as input for the computation of the GENEPY values. Values refer to year 2017. In panel (b), time series of the correlation coefficients among the GENEPY values computed using as input for the algorithm the binary matrix M and the ones obtained using as input the RCA matrix. The correlation coefficients are of the Pearson's kind.

SUPPLEMENTARY FIGURE 11

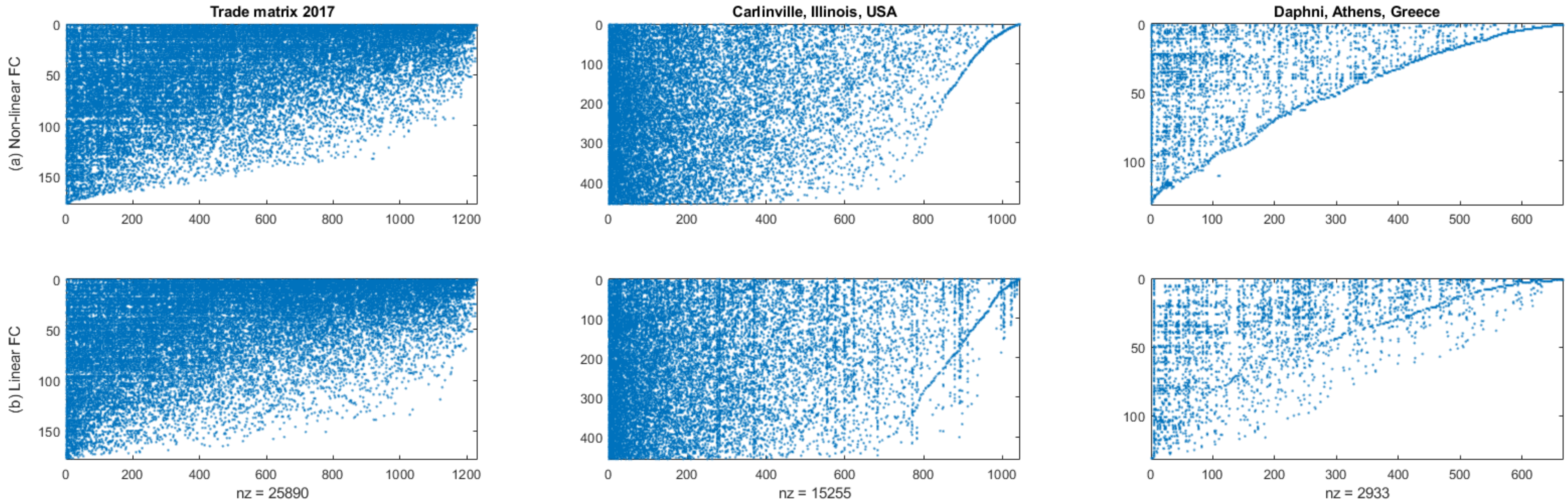

Nestedness maximization performances. Visual comparison among the performances of the non-linear FC algorithm (panels (a)) and its linearized form, (panels (b)) in maximizing nestedness of matrices. The left panels refer to the countries-products bipartite network during 2017. The central panels refer to the network of pollination in Carlinville, Illinois, USA (network ID: M_PL_062); on the right the one referring to the pollination in Daphní, Athens, Greece (network ID: M_PL_015). Data for the pollination networks are freely available at www.web-of-life.es.

SUPPLEMENTARY TABLE 1

Ranking positions of countries according to ascending values of GENEPY. Results refer to year 2017.

Ranking position	Country iso-3 code	Country name	Ranking position	Country iso-3 code	Country name	Ranking position	Country iso-3 code	Country name
1	JPN	Japan	60	VGB	British Virgin Islands	119	CUQ	Curaçao
2	KOR	Korea, Rep. of Korea	61	COL	Colombia	120	SLE	Sierra Leone
3	DEU	Germany	62	LBN	Lebanon	121	RWA	Rwanda
4	CHE	Switzerland-Liechtenstein	63	PRK	Korea, Dem. People's Rep. of	122	TGO	Togo
5	USA	United States of America	64	PAK	Pakistan	123	NIC	Nicaragua
6	CHN	China	65	URY	Uruguay	124	ETH	Ethiopia
7	CZE	Czech Republic	66	LKA	Sri Lanka	125	MOZ	Mozambique
8	GBR	United Kingdom	67	ARG	Argentina	126	SAU	Saudi Arabia
9	HKG	Hong Kong (SARC)	68	BRB	Barbados	127	TJK	Tajikistan
10	SWE	Sweden	69	KHM	Cambodia	128	BDI	Burundi
11	SGP	Singapore	70	MKD	The former Yugoslav Rep. of Macedonia	129	BTN	Bhutan
12	AUT	Austria	71	MDA	Moldova, Rep.of	130	KWT	Kuwait
13	ITA	Italy	72	KGZ	Kyrgyzstan	131	BEN	Benin
14	MYS	Malaysia	73	JOR	Jordan	132	MWI	Malawi
15	BEL	Belgium-Luxembourg	74	UZB	Uzbekistan	133	GHA	Ghana
16	ISR	Israel	75	SYR	Syrian Arab Republic	134	CMR	Cameroon
17	THA	Thailand	76	KAZ	Kazakstan	135	AZE	Azerbaijan
18	FRA	France	77	MUS	Mauritius	136	CUB	Cuba

Ranking position	Country iso-3 code	Country name	Ranking position	Country iso-3 code	Country name	Ranking position	Country iso-3 code	Country name
19	NLD	Netherlands	78	CRI	Costa Rica	137	CIV	Côte d'Ivoire
20	FIN	Finland	79	AUS	Australia	138	TTO	Trinidad and Tobago
21	SVN	Slovenia	80	MNE	Montenegro	139	GIB	Gibraltar
22	SVK	Slovakia	81	CHL	Chile	140	BHS	Bahamas
23	HUN	Hungary	82	DOM	Dominican Republic	141	COD	Democratic Republic of the Congo
24	POL	Poland	83	PER	Peru	142	SDN	Sudan (2011)
25	PHL	Philippines	84	ARE	United Arab Emirates	143	DZA	Algeria
26	IRL	Ireland	85	ARM	Armenia	144	TKM	Turkmenistan
27	IND	India	86	ALB	Albania	145	MHL	Marshall Islands
28	ESP	Spain	87	ABW	Aruba	146	NER	Niger
29	DNK	Denmark	88	MMR	Myanmar	147	GMB	Gambia
30	ROU	Roumania	89	MAR	Morocco	148	GUY	Guyana
31	MEX	Mexico	90	SYC	Seychelles	149	NCL	New Caledonia
32	HRV	Croatia	91	BGD	Bangladesh	150	PNG	Papua New Guinea
33	EST	Estonia	92	FJI	Fiji	151	BRN	Brunei Darussalam
34	IDN	Indonesia	93	PRY	Paraguay	152	VEN	Venezuela
35	VNM	Viet Nam	94	ISL	Iceland	153	SUR	Suriname
36	LTU	Lithuania	95	KEN	Kenya	154	NGA	Nigeria
37	PRT	Portugal	96	GEO	Georgia	155	BFA	Burkina Faso
38	TUR	Turkey	97	BHR	Bahrain	156	SOM	Somalia
39	BLR	Belarus	98	ATG	Antigua and Barbuda	157	ERI	Eritrea
40	BRA	Brazil	99	MDG	Madagascar	158	COG	Congo
41	CYP	Cyprus	100	JAM	Jamaica	159	YEM	Yemen
42	BGR	Bulgaria	101	LAO	Lao People's Democratic Republic	160	GIN	Guinea
43	LVA	Latvia	102	GTM	Guatemala	161	QAT	Qatar
44	CAN	Canada	103	HND	Honduras	162	LBR	Liberia
45	NOR	Norway	104	UGA	Uganda	163	VUT	Vanuatu
46	UKR	Ukraine	105	OMN	Oman	164	SLB	Solomon Islands

Ranking position	Country iso-3 code	Country name	Ranking position	Country iso-3 code	Country name	Ranking position	Country iso-3 code	Country name
47	TUN	Tunisia	106	SEN	Senegal	165	GAB	Gabon
48	RUS	Russian Federation	107	IRN	Iran (Islamic Republic of)	166	MRT	Mauritania
49	SRB	Serbia	108	BLZ	Belize	167	FLK	Falkland Islands (Malvinas)
50	NPL	Nepal	109	ZMB	Zambia	168	GRL	Greenland
51	MAC	Macau	110	MNG	Mongolia	169	TCD	Chad
52	SLV	El Salvador	111	HTI	Haiti	170	CYM	Cayman Islands
53	ZAF	South Africa	112	BOL	Bolivia	171	MDV	Maldives
54	MLT	Malta	113	VCT	Saint Vincent and the Grenadines	172	LBY	Libyan Arab Jamahiriya
55	BIH	Bosnia and Herzegovina	114	ZWE	Zimbabwe	173	AGO	Angola
56	EGY	Egypt	115	AFG	Afghanistan	174	GNB	Guinea-Bissau
57	GRC	Greece	116	ECU	Ecuador	175	SSD	South Sudan
58	NZL	New Zealand	117	TZA	Tanzania, United Rep. of	176	IRQ	Iraq
59	PAN	Panama	118	MLI	Mali	177	GNQ	Equatorial Guinea

SUPPLEMENTARY NOTES

SUPPLEMENTARY NOTE 1: IMPLEMENTATION OF THE ALGORITHMS

The two algorithms of economic complexity, i.e., the *Method of Reflection*, MR, and the *Fitness and Complexity* algorithm, FC, have been separately implemented following the steps presented in Sect. *Methods*. In order to prevent divergence to null or infinite values, our implementation of the FC algorithm in Eqs 11 of the main text includes the convergence criteria adopted in (1): the algorithm stops at the iteration *N*, when the rankings between step *N* and step *N+ΔN*, have a Spearman's correlation coefficient larger than *0.999*, in this way ensuring *rank convergence* of the algorithm. In this work we assumed *ΔN=10.*

Small divergences of the results with respect to the official ones provided by the World Bank (2) – for the Fitness values – and from the Observatory of Economic Complexity (3) – for ECI – should be attributed to either different sanitation procedure of the data, also considering the larger number of countries here accounted for, *or* differences in the convergence criteria adopted for the FC algorithm.

SUPPLEMENTARY NOTE 2: THE COMPLEXITY OF PRODUCTS

Supplementary Figures 4 – 5 show the results of the GENEPY index for products. In Supplementary Fig. 4, panel (b), higher correlation is found among $Y_{p,1}$ and the term $Q_p k'_p$, in fact we showed how the first eigenvector $Y_{p,1}$ solves the problem of finding linearly computed Quality values, as expected. Lower correlation is found when comparing the values of the second eigenvectors $Y_{p,2}$ with the values $PCI_p \sqrt{k_p}$, panel (c), due to the differences among the matrix $W^A_{cp} = M_{cp}/ \sqrt{k_c}\sqrt{k_p}$, from which we are able to recover the exact metrics ECI and PCI, and the matrix $W^B_{cp} = M_{cp}/k_c\, k'_p$, which are here used to compute the GENEPY (hence $Y_{p,1}$ and $Y_{p,2}$) values. In Supplementary Fig. 5, differences in the complexity computed according to the GENEPY index among the categories clearly emerge: commodities into the *Machinery* or *Electrical* categories naturally require different and more sophisticated knowledge in order to be produced, while resource-based commodities, such as *Animals* or *Foodproducts* do not need special knowledge requirements in order to be produced or traded. In addition, the GENEPY values may vary widely in some categories such as *Chemicals*, where the natural availability of natural resources and the requirements for their extraction may define the need for higher complex technologies for making these available for trade.

SUPPLEMENTARY NOTE 3: THE KNEE-LIKE SHAPE

The knee-shape of the points in the plane $X_{c,1} - X_{c,2}$ is recurrent in all the years of analysis, thus showing the existence of a functional relationship between the two eigenvectors. The reasons of the knee-like shape of this functional relationship are related to linear algebra and network science.

Let us define a functional relationship f between $X_{c,1}$ and $X_{c,2}$ s.t.

$$X_{c,2} = f\left(X_{c,1}\right) + \epsilon_c, \qquad \text{(Eq 1)}$$

where ϵ_c are the errors. We assume the errors to have null expected value, i.e., $\mathrm{E}(\epsilon_c) = 0$ and to be orthogonal to $X_{c,1}$, s.t., $\sum_c X_{c,1}\epsilon_c = 0$.

There exist some constraints related to the existence of the eigenvectors of a symmetric matrix, which any functional relationship should respect:

(i) the eigenvectors corresponding to distinct eigenvalues of a symmetric squared matrix are, by definition, orthogonal and this entails that the inner product of the vectors is zero, i.e., $\sum_c X_{c,1} \cdot X_{c,2} = 0$;

(ii) for the Perron-Frobenius theorem, the eigenvector corresponding to the largest eigenvalue is strictly positive, s.t. $X_{c,1} \geq 0 \; \forall \; c = 1, \ldots, C$ (number of countries);

(iii) we can normalize the eigenvectors such that the 2-norm is unitary, i.e., $\sum_c X_{c,1}^2 = \sum_c X_{c,2}^2 = 1$;

(iv) if any element of the eigenvector corresponding to the first (largest) eigenvalue λ_1 is zero, the same element is null also within the successive eigenvectors. In fact, the eigen-equation for the matrix N is:

$$X_{c^*,1}\lambda_1 = \sum_c N_{cc^*} X_{c,1} \, ;$$

because of condition (ii), it holds that $X_{c^*,1} = 0$ iff $\sum_c N_{cc^*} = 0$, i.e., if the matrix has null elements all along the column (or row) c^*. Interpreting this result through network science lenses, the node to which the null element of the eigenvector refers is disconnected in the network. Therefore, in the hypothesis of existence of any functional relationship between two eigenvectors as in Eq 1, it must hold $f(0) = 0$.

We now proceed exploring two cases of possible functional relationship for Eq 1.

CASE A: The simplest form of this relation considers f as a linear function, i.e.,

$$X_{c,2} = aX_{c,1} + \epsilon_c \qquad \text{(Eq 2)}$$

By imposing the orthogonality condition (i) to Eq 2 one obtains:

$$\sum_c X_{c,1} X_{c,2} = \sum_c X_{c,1}(aX_{c,1} + \epsilon_c) = a \sum_c X_{c,1}^2 + \sum_c X_{c,1}\epsilon_c = 0$$

Since the errors are orthogonal to $X_{c,1}$ and the 2-norm of the vector is unitary for condition (iii), the solution is $a = 0$, which entails no functional relationship exists between $X_{c,1}$ and $X_{c,2}$.

CASE B: We consider the function to be polynomial of the second order, namely:

$$X_{c,2} = aX_{c,1} + bX_{c,1}^2 + \epsilon_c \qquad \text{(Eq 3)}$$

Again, by applying the orthogonality condition (i), one has:

$$\sum_c X_{c,1} X_{c,2} = \sum_c X_{c,1}(aX_{c,1} + bX_{c,1}^2 + \epsilon_c) = a \sum_c X_{c,1}^2 + b \sum_c X_{c,1}^3 + \sum_c X_{c,1}\epsilon_c = 0$$

which leads to

$$a + b\sum_c X_{c,1}^3 = 0 \qquad \text{(Eq 4)}$$

Because of condition (ii), the term $\sum_c {X_{c,1}}^3$ is strictly positive and in order to respect Eq 4, the values of the parameter a and b should have different signs, thus justifying the existence of the knee-like shape. In particular, the upward belly of the relation is given for negative values of the parameter a and positive values of b. In this sense, the minimum point depends on the parameters.

We can read this result through the meaning of the matrix and its eigenvectors in the context of network theory. In fact, in this case the eigenvectors of the matrix describe the structural properties of the network (4) and are related to the similarity of the network among the countries. In fact, the shape of the matrix N (Figure S4 of this SI), represents a connected network in which a stronger connected component can be spotted, constituted by the top-GENEPY countries, while weaker connections characterize the countries at the periphery. In this weak connection component, as shown in (5), the correlation between the two eigenvectors is positive. Also, as stated by the authors in (5), the mutual signs of the elements of the eigenvectors corresponding to the two largest eigenvalues – whether these are positive or negative in the second eigenvector – acquires a meaning, thus justifying the presence of three areas (or groups) in which the points can stand:

i) both values $X_{c,1}$ and $X_{c,2}$ are low: these nodes belong to the weaker component and they have no important connections with the strongest connected component;

ii) both values $X_{c,1}$ and $X_{c,2}$ are high: these nodes belong to the strongest and more connected core of the network, thus defining the area in which these points (countries) are competitors, also in the sense of collecting most of the links in terms of similarities;

iii) low values of $X_{c,1}$, high values of $X_{c,2}$ or viceversa: this situation identifies the presence of some "outliers" of the core and the periphery components. These nodes connect the stronger and the weaker components and have a role in bridging the gaps across the network. We identify these nodes as able to jump, during time, from one group to another.

These three behaviors along the knee-like shape evolve in time, letting the dynamical regimes of growth *Impasse, Bounce* and *Arena,* emerge as we analyse the aggregated dynamics of countries in time.

SUPPLEMENTARY NOTE 4: THE REGIMES OF GROWTH

An analysis of the trajectories of countries according to their values in $X_{c,1}$ and $X_{c,2}$ allows one distinguishing the presence of the three regimes of growth along the knee-like shape: *Impasse, Bounce* and *Arena.*

For each country whose continuous data in time are available (154 countries), we defined the main displacement recorded by the country identifying a starting and an ending point during the period of analysis. We connect the point located at the center of mass of $\mathrm{X}_{c,1}$ and $\mathrm{X}_{c,2}$ during the first 3 years of analysis (1995 – 1998) to the center of mass during the last 3 years (2014 – 2017). In order to make the overall dynamics clearer, we defined overlapping classes of countries using a moving window of 20 countries per each class. Firstly, we ordered the countries (and respective scores of the eigenvectors in time) for increasing starting $\mathrm{X}_{c,1}$ values.

Secondly, by defining each class through a window of 20 countries, we computed the resultant vector of the displacements of the countries falling in that class. Lastly, we applied the resultant vectors to the barycenter of the starting points of the single vectors that fall into the class.

In Supplementary Figure 9, we show the aggregated dynamics of countries along the knee-shape. The colours sort the vectors for their length, as normalized for the longest vector recorded (light blue identifies the shorter ones, light purple the longer ones). The light blue vectors on the bottom left part of the knee identify the *Impasse*: the dynamics of the countries in this area are here tangled, as shown by the horizontal displacement of the vectors. Notwithstanding the presence of some uplift movements of the classes around the minimum point in $X_{c,1} = 0.05$, the countries within this area are stacked in this dynamic of poor diversification and complexity within the cluster of lower growth. As soon as countries reinforce their knowledge, the countries experience higher values of $X_{\mathrm{c},2}$ until these values approach to zero: here it starts the *Bounce*, where countries boost their diversification and complexity, turning cluster membership by joining the more economically grown countries club and thus increasing the similarity in the export basket with them. Longer vectors in violet and light purple highlight the jump. Once the economies have experienced the boost, they join the *Arena* of competition, for which continuous growth is determined. It is interesting to observe a divergent direction in the highest part of the Arena (high values of $X_{c,1}$ and $X_{c,2}$). Here, countries may lose ground on the plane of growth. Many factors may contribute to this downgrading dynamic. In fact, as described in the main article, the economic and financial crisis are more likely to be the cause of these drops; also, the entrance in the markets of new economies decreases the potential of economies to increase their economic complexity in time.

SUPPLEMENTARY NOTE 5: ECOLOGICAL NETWORKS

As detailed in the Discussion, the very similar results between the linear and the non-linear versions of the FC algorithm cannot be generalised to other systems. In fact, non-linearity has been shown to be an important feature of the algorithms for temperature minimization and the FC algorithm has very good potential in minimizing the nestedness temperature of ecological networks (1). Therefore, we have tested the packing performance of the linearized form of the FC algorithm, similarly to the comparison showed in (1). We exemplify the results through the analysis of two pollination networks provided by The Web of Life project and available at www.web-of-life.es (network IDs : M_PL_062 and : M_PL_015). The networks describe the pollination phenomena among plants and pollinators. As Supplementary Figure 11 shows, the non-linear algorithm outperforms the linearised form in its capability of maximizing the nestedness of the incidence matrices of the two pollination. Instead, there are no significant differences between the non-linear and the linear algorithm for maximising the data-packing of the trade matrix, confirming that the feature of linearity pertains to the countries-products bipartite network as far as explored.

SUPPLEMENTARY REFERENCES

1. **Lin, J. H., Tessone, C. and Mariani, M.** Nestedness maximization in complex networks through the fitness-complexity algorithm. 2018.

2. **Tacchella, A., et al.** Economic Fitness - The World Bank. [Online] 2018. datacatalog.worldbank.org/dataset/economic-fitness.

3. **Hidalgo, C. A. and Hausmann, R.** The Observatory of Economic Complexity. [Online] 2018. oec.world/en/.

4. **Newman, M. E.** Spectral methods for community detection and graph partitioning. 2013, Vol. 88, 4.

5. **Lucińska, M., & Wierzchoń, S. T.** Clustering based on eigenvectors of the adjacency matrix. *International Journal of Applied Mathematics and Computer Science.* 2018, 28.

6. **World Integrated Trade Solutions.** *WITS - World Bank.* [Online] wits.worldbank.org.

7. **Mealy, P., Farmer, J. D., & Teytelboym, A.** Interpreting economic complexity. 2019, Vol. 51, 1.